SUPPLEMENTAL MATERIALS

Trans-right-ventricle and transpulmonary metabolite gradients in human pulmonary arterial hypertension

Philippe Chouvarine[1], Martin Giera[2], Gabi Kastenmüller[3], Anna Artati[4], Jerzy Adamski [5,6], Harald Bertram[1], Georg Hansmann[1,*]

[1] Department of Pediatric Cardiology and Critical Care, Hannover Medical School, Hannover, Germany
[2] Center for Proteomics and Metabolomics, Leiden University Medical Center, Leiden, The Netherlands
[3] Institute of Bioinformatics and Systems Biology, Helmholtz Zentrum München, Deutsches Forschungszentrum für Gesundheit und Umwelt, Neuherberg, Germany
[4] Institute of Experimental Genetics, Genome Analysis Center, Helmholtz Zentrum München, Deutsches Forschungszentrum für Gesundheit und Umwelt, Neuherberg, Germany
[5] Research Unit Molecular Endocrinology and Metabolism, Genome Analysis Center, Helmholtz Zentrum München, Deutsches Forschungszentrum für Gesundheit und Umwelt, Neuherberg, Germany
[6] Department of Biochemistry, Yong Loo Lin School of Medicine, National University of Singapore, Singapore

*** Corresponding author:**

Prof. Dr. Georg Hansmann, MD, PhD, FESC, FAHA
Department of Pediatric Cardiology and Critical Care
Hannover Medical School
Carl-Neuberg-Str. 1
30625 Hannover
Germany
E-mail: georg.hansmann@gmail.com

SUPPLEMENTARY INTRODUCTION

Invasive assessment of right and left heart hemodynamics is mandatory for diagnosis of pulmonary hypertension (PH) and its classification (PAH is WHO group 1 PH). [1, 2] In addition, transthoracic echocardiography is a readily available, easy to use method to evaluate RVH, dilation and systolic function non-invasively.[3] Several invasive-hemodynamic, echocardiographic and clinical variables can be used in combination to estimate patient risk and prognosis, and to determine the best PAH therapy.[2, 4] However, due to heterogeneous etiologies of PAH and confounding factors such as variable preload (volume status) and inter-observer variability, reliance on non-invasive hemodynamic variables alone is problematic.[1]

Sole right heart catheterization is frequently performed at PH centers, so that, most of the above studies used either peripheral arterial blood[5] or even pulmonary arterial wedge specimen[6, 7, 8] as “post lung samples”. Due to the very high variability of such circulating “remote post lung markers”, statistical power, result interpretation, and conclusions were limited.

A few studies identified venous metabolites as potential biomarkers for PAH[9, 10] or CVD-related mortality.[11] In the largest study, investigators measured plasma concentrations of 1416 circulating metabolites in peripheral venous blood, and found that 53 of those metabolites distinguished adult PAH patients from healthy controls.[9] In a separate study, plasma samples obtained by right heart catheterization and radionuclide ventriculography from PAH patients were screened for 105 metabolites by targeted mass spectrometry: 21 were identified as indicators of right ventricular-pulmonary vascular dysfunction.[10]

SUPPLEMENTARY METHODS

1. Cardiac Catheterization

For the purpose of this prospective study, pediatric PAH was defined as per 2015/2016 international guidelines[2, 4, 12]: mean pulmonary artery pressure (mPAP) ≥25 mmHg, a pulmonary arterial wedge pressure (PAWP) ≤15 mm Hg, and pulmonary vascular resistance index (PVRi) >3 WU·m^2 when >3 months old, at sea level. PAH and non-PAH patients of both genders, more than 3 months and less than 18 years old, were enrolled and underwent combined right and left heart catheterization.

The most recent World Symposium on PH (WSPH) in Nice (2018) decreased the cut-off value for mean pulmonary arterial pressure, so that PAH was defined as mPAP > 20 mmHg at rest.[13, 14] PAH is a subgroup of PH in which pre-capillary PH is dominating, defined as combination of a mPAP > 20 mmHg, a pulmonary arterial wedge pressure (PAWP) ≤15 mm Hg (alternatively: LV end-diastolic pressure or mean left atrial pressure), and a pulmonary vascular resistance (PVR) >3 Wood units (WU) (in children: PVR index >3 WU·m^2 when >3 months old, at sea level).[2, 4, 14, 15, 16, 17]

All patients underwent right and left heart catheterization in room air, under conscious intravenous sedation (propofol) and local anesthesia for femoral access (2 venous sheaths, 1 arterial sheath), with the exception of patients 7 and 8 in the Metabolon study (6.6 kg and 4.5 kg) who had Trisomy 21 and had to be intubated and mechanically ventilated. Three catheters were positioned in the SVC, right or left pulmonary artery (wedge catheter), and the ascending aorta (pigtail catheter; **Fig.1**). Arterial blood gas analysis confirmed normoventilation. Once these catheter positions were stably achieved, pressure recordings, blood gas analyses and EDTA blood samples were obtained near-simultaneously within one minute. Pulmonary blood flow and cardiac index were calculated by applying the Fick principle.

2. Transthoracic echocardiography

All patients underwent transthoracic echocardiography (iE33, Philips) on the day preceding the cardiac catheterization following a standardized protocol.[3]

3. Blood plasma collection

EDTA blood was spun down at 1300g and room temperature for 10 minutes, within 20 minutes after sample collection. Plasma was then aliquoted in 500 µl aliquots and immediately frozen at -80°C. After thawing, plasma samples underwent a high speed spin step at 18,000g, 4°C for 15 minutes.

4. Non-targeted metabolite measurements

Plasma samples were stored at -80 °C prior to analysis at Helmholtz Zentrum München, Germany. On the day of extraction, samples were thawed on ice, were randomized, and were distributed into 3 batches. A hundred µL of the plasma were pipetted into a 2 mL 96-well plate. In addition to samples from this study, a pooled human reference plasma sample (Seralab, West Sussex, UK) were extracted as samples of the study and placed 7 wells of each batch. These samples served as technical replicates throughout the data set to assess process variability. Besides those samples, 100 µL of water was extracted as samples of the study and placed in 6 wells of each 96-well plate to serve as process blanks.

Protein was precipitated and the metabolites in the plasma samples were extracted with 475 µL methanol, containing four recovery standard compounds to monitor the extraction efficiency. After centrifugation, the supernatant was split into 4 aliquots of 100 µL each onto two 96-well microplates. The first 2 aliquots were used for LC-MS/MS analysis in positive and negative electrospray ionization mode. Two further aliquots on the second plate were kept as

a reserve. The samples were dried on a TurboVap 96 (Zymark, Sotax, Lörrach, Germany). Prior to LC-MS/MS in positive ion mode, the samples were reconstituted with 50 µL of 0.1% formic acid and those analyzed in negative ion mode with 50 µL of 6.5 mM ammonium bicarbonate, pH 8.0. Reconstitution solvents for both ionization modes contained further internal standards that allowed monitoring of instrument performance and also served as retention reference markers. To minimize human error, liquid handling was performed on a Hamilton Microlab STAR robot (Hamilton Bonaduz AG, Bonaduz, Switzerland).

LC-MS/MS analysis was performed on a linear ion trap LTQ XL mass spectrometer (Thermo Fisher Scientific GmbH, Dreieich, Germany) coupled with a Waters Acquity UPLC system (Waters GmbH, Eschborn, Germany). Two separate columns (2.1 x 100 mm Waters BEH C18 1.7 µm particle) were used for acidic (solvent A: 0.1% formic acid in water, solvent B: 0.1% formic acid in methanol) and for basic (A: 6.5 mM ammonium bicarbonate pH 8.0, B: 6.5 mM ammonium bicarbonate in 95% methanol) mobile phase conditions, optimized for positive and negative electrospray ionization, respectively. After injection of the sample extracts, the columns were developed in a gradient of 99.5% A to 98% B in 11 min run time at 350 µL/min flow rate. The eluent flow was directly connected to the ESI source of the LTQ XL mass spectrometer. Full scan mass spectra (80 – 1000 m/z) and data dependent MS/MS scans with dynamic exclusion were recorded in turns. Metabolites were annotated by curation of the LC-MS/MS data against proprietary Metabolon's chemical database library (Metabolon, Inc., Durham, NC, USA) based on retention index, precursor mass and MS/MS spectra. In this study, 427 metabolites, 289 compounds of known identity (named biochemical) and 138 compounds of unknown structural identity (unnamed biochemical) were identified. The unknown chemicals are indicated by a letter X followed by a number as the compound identifier. The metabolites were assigned to cellular pathways based on PubChem, KEGG, and the Human Metabolome Database.

5. Untargeted lipidomics

Lipidomics analysis was carried out on the commercial Lipidyzer platform, according to the manufacturer's instructions (Sciex).[18, 19] Lipid analysis was performed after methyl-tert.-butyl ether extraction[20] in flow-injection mode, separating lipid classes by differential mobility spectroscopy,[18] followed by tandem mass spectrometry of lipid species with a QTrap 5500 operated in multiple reaction monitoring mode. Lipid species were identified and quantified on the basis of characteristic mass spectrometric transitions. Commercial Lipidyzer software automatically calculated lipid species concentrations. All samples were analyzed in a randomized fashion. Control plasma samples, as well as fortified plasma samples, were assessed daily as quality controls. Relative standard deviations of quality control samples were below 15% for all lipid classes, except for sphingomyelin, for which a relative standard deviation of 25% was noted. In summary, the Lipidyzer is a validated quantitative lipidomics platform allowing the selective and quantitative analysis of 836 individual lipid species. It allows an unprecedented detailed view of the plasma lipidome in our study cohort, thereby providing highly orthogonal and complementary information to the Metabolon platform used in our clinical investigation.

6. Statistical analysis (Metabolon study, metabolomics)

Metabolites with a missing value in at least one of the three catheterization sites were removed from the gradient analysis. For the trans-RV and transpulmonary gradient analysis we used mixed effects models with log2 of fold change (FC) between two catheterization sites (PA vs. SVC for the trans-RV gradient and AAO vs. PA for the trans-pulmonary gradient) as the dependent variable, groups (PAH or Control) as an independent variable, and each patient as a random effect (log2(FC)~Group, random=~1|Patient). To avoid technical artifacts, iterative outlier removal procedure for the outliers identified using Grubb's test (p-val>0.1) was applied to log2 of the relative ion count values at each of the two

catheterization sites prior to modeling. Following the outlier removal, metabolites with less than three control or four PAH FCs were removed. The generated models were evaluated using the Anova function from the car R package, and the p-values generated by Type II Wald chi-square test (using the "car" R package[21]) were further corrected for multiple testing following the modified FDR procedure described in Li et al.[22] The three between group comparisons at each catheterization site were performed using Mann-Whitney U test after the iterative outlier removal procedure for the outliers identified using Grubb's test (p-val>0.1) was applied to the values of a given catheterization site. The same modified FDR multiple testing correction[22] was performed.

For each experimental setting described above we performed principal component analysis (PCA) aiming to show how well all metabolites in our analyses are able to discriminate phenotype (PAH vs. non-PAH). The PCA was performed on the preprocessed data for each comparison (as described above). The results showing the first two principal components are presented in **Fig. S1**.

Metabolite ratios were created such that numerator contained significantly differentially concentrated metabolites (FDR<0.15) and all respective denominators contained neighboring nodes with distance ≤ 2 from a network of human metabolites (a combination of knowledge-based Recon network and data-driven Metabolon network). The resulting ratios underwent the same analysis as single metabolites. In most cases the ratios had smaller differences (effect sizes) compared to the respective single metabolite. However, in the case of the 1-stearoyl-GPI (18:0) / 10-heptadecenoate (17:1n7) ratio in the PA, the fold change increased to 4.52, compared to 3.85 for 1-stearoyl-GPI (18:0) alone. Besides this exception, the above ratio analysis in our study did not produce significantly better correlations of metabolites with hemodynamic/echocardiographic variables.

Metabolites and ratios with low adjusted p-values were correlated with hemodynamics. The trans-RV and trans-pulmonary gradient fold changes (log2(FC)) were

correlated using Pearson's r. The relative ion counts of the significantly differentially expressed (PAH vs Control) metabolites within one of the catheterization sites were correlated with hemodynamic values using Spearman's rho.

Network analysis presented below was performed by calculating second-order Pearson's correlations for the fold changes in the gradient analysis and Spearman's correlations for the normalized ion counts in the between group analysis in the SVC and PA. The networks were visualized using the MetScape Cytoscape application.

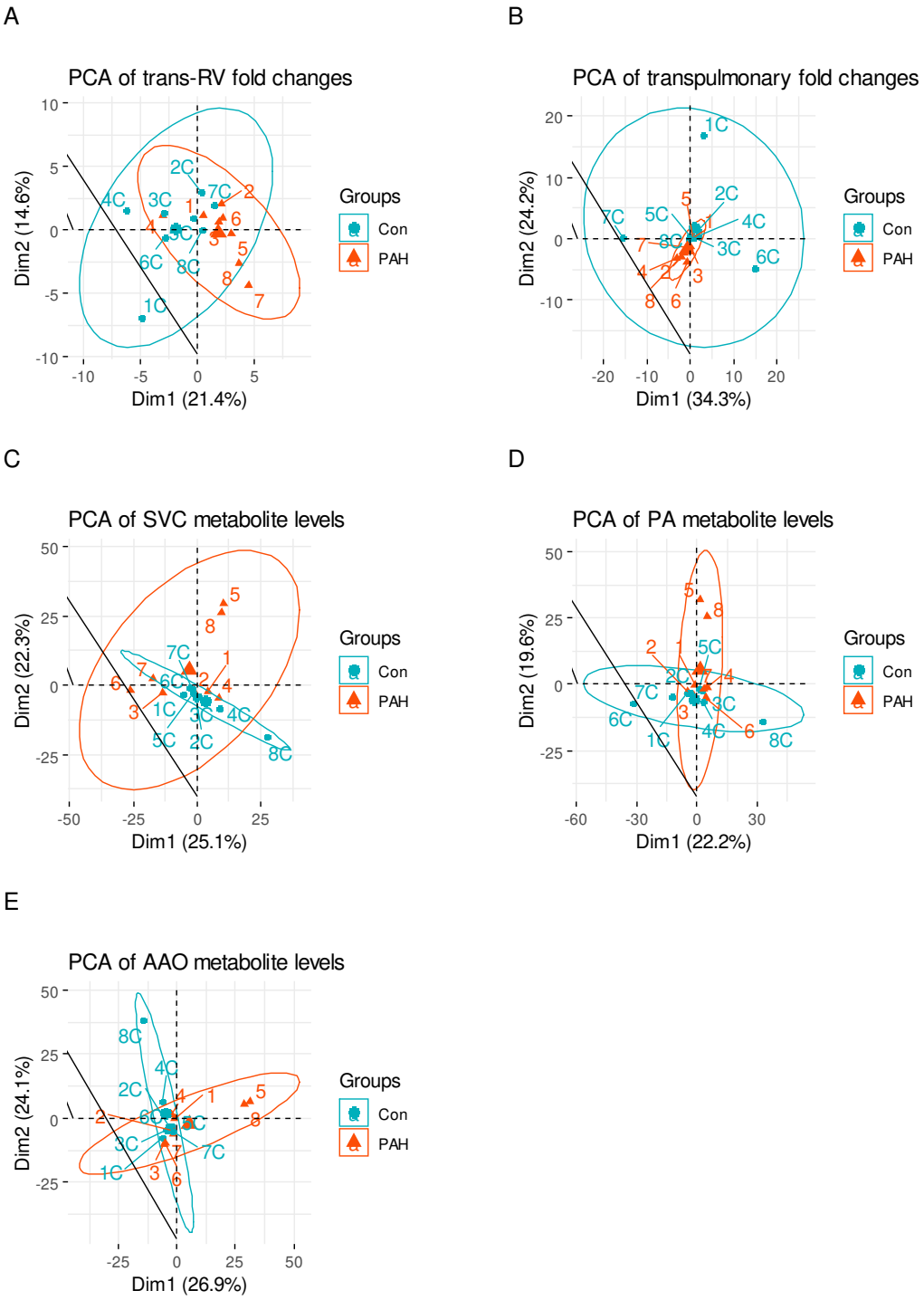

Figure S1. Principal component analysis of metabolite variability in each experimental setting: (A) trans-RV gradient, (B) transpulmonary gradient, (C) superior vena cava, (D) pulmonary artery, (E) ascending aorta.

Metabolite concentration correlation network analysis

To identify regulatory hubs with the most impact on the identified differentially concentrated metabolites in each experimental setting (trans-RV, transpulmonary, or between group comparisons in a single catheterization site), we performed network analysis based on the second-order correlations among the differentially concentrated metabolites with a p-value<0.05 (prior to the FDR adjustment), as described above. The results of the analysis revealed that in the trans-RV, none of the gradients formed a noticeable "hub" node that would exert influence on multiple neighboring metabolites in this correlation-driven network (**Fig. S2 A**). The highest degree nodes in the trans-RV setting represented 1-palmytoyl GPE (16:0), pyroglutamine, and arachidate (20:0), each of which correlated with three other metabolites ($r \geq 0.40$). Among the transpulmonary gradients, arachidonate (20:4n6) stood out as a "hub" node with second-order correlations ($r \geq 0.40$) to five other metabolites, however the correlations were only moderate ($0.40 \leq r \leq 0.49$) (**Fig. S2 B**). This influence of arachidonic acid (arachidonate (20:4n6)) is expected, given the central role it plays in eicosanoid metabolism (further discussed in the "Discussion of selected metabolites with differential transpulmonary gradients (Trans-PC gradients)" section below). In the single site comparisons the noticeable "hub" metabolites were taurodeoxycholate (4 correlations, $0.42 \leq rho \leq 0.50$) and heptanoate (7:0) (4 correlations, $0.40 \leq rho \leq 0.51$) in the SVC (**Fig. S2 C**), and 1-(1-enyl-palmitoyl)-GPE (P-16:0) (4 correlations, $0.43 \leq rho \leq 0.51$ and $rho = -0.50$) in the PA (**Fig. S2 D**).

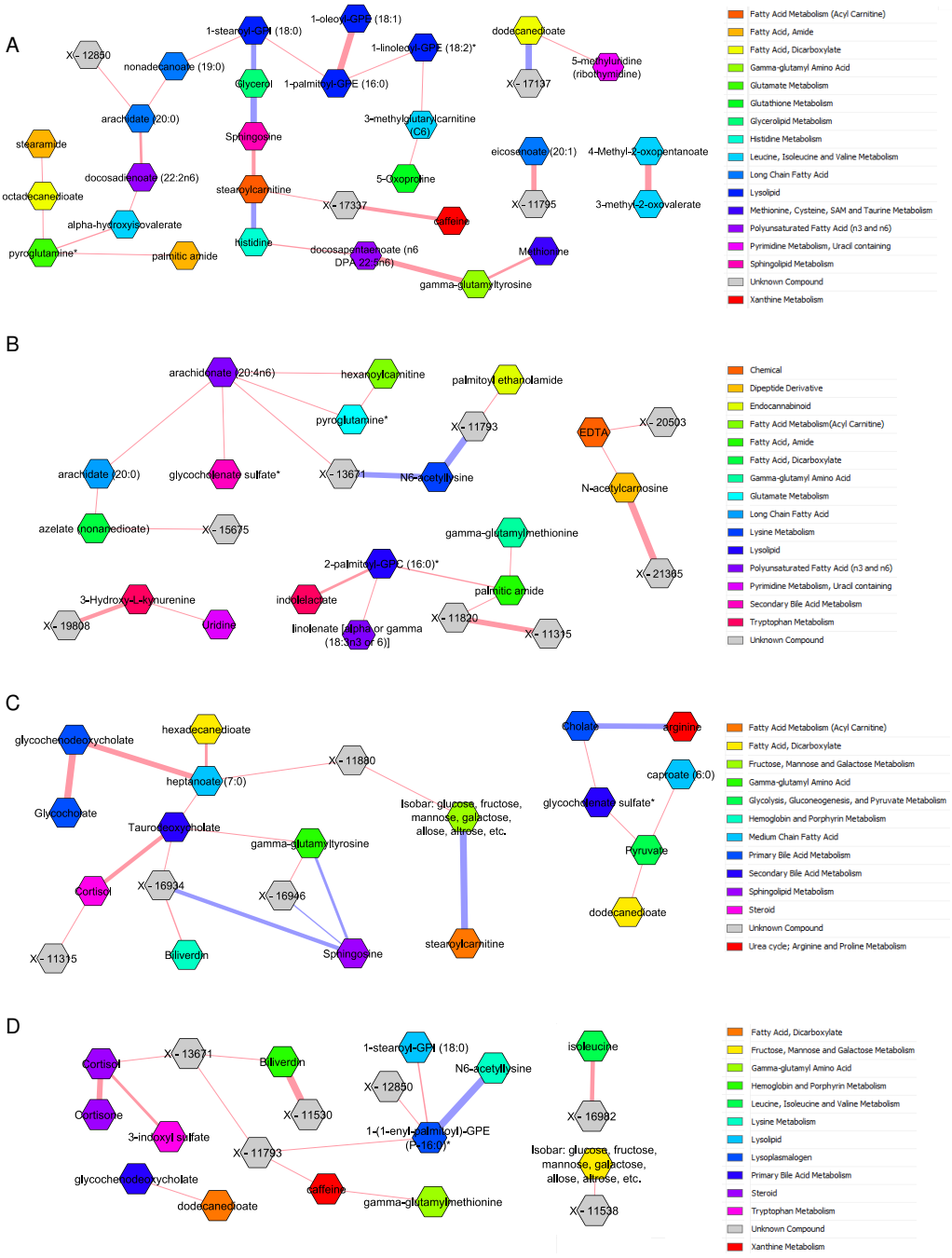

Figure S2. Metabolites exerting the most influence are identified as "hub" nodes using network analysis based on the second-order correlations among the differentially concentrated metabolites (PAH vs. controls; p-val<0.05, without FDR correction). Positive correlations are shown in red, negative correlations are shown in blue. The line thickness indicates correlation strength. Metabolites without a single correlation ($r \leq -0.4$ or $r \geq 0.4$; rho ≤ -0.4 or rho ≥ 0.4, for single sites, i.e. C and D) were excluded. (A) Network of differential trans-RV gradients based on fold changes (PA vs. SVC) of 32 metabolites. (B) Network of differential transpulmonary gradients based on fold changes (AAO vs. PA) of 26 metabolites. (C) Network of differentially concentrated metabolites in the SVC based on normalized ion counts of 24 metabolites. (D) Network of differentially concentrated metabolites in the PA based on normalized ion counts of 20 metabolites.

7. Statistical analysis (Lipidyzer study; lipidomics)

We followed the same statistical analysis methodology for analysis of lipids species and fatty acid (FA) concentrations obtained from the Lipidyzer platform. The only exception was not using the log2 transformation in the outlier removal procedure, since the raw data was normally distributed. We also did not perform separate ratio analysis, since the ratios were already included in the output. Correlation network analysis was also omitted, since the Lipidyzer experiments were meant to be used as support for metabolite profiling study described above.

For each experimental setting we performed principal component analysis (PCA) aiming to show how well all lipid species and FAs in our analyses are able to discriminate the phenotypes (PAH vs. non-PAH). The PCA was performed on the preprocessed data for each comparison (as described above). The results showing the first two principal components are presented in **Fig. S3**.

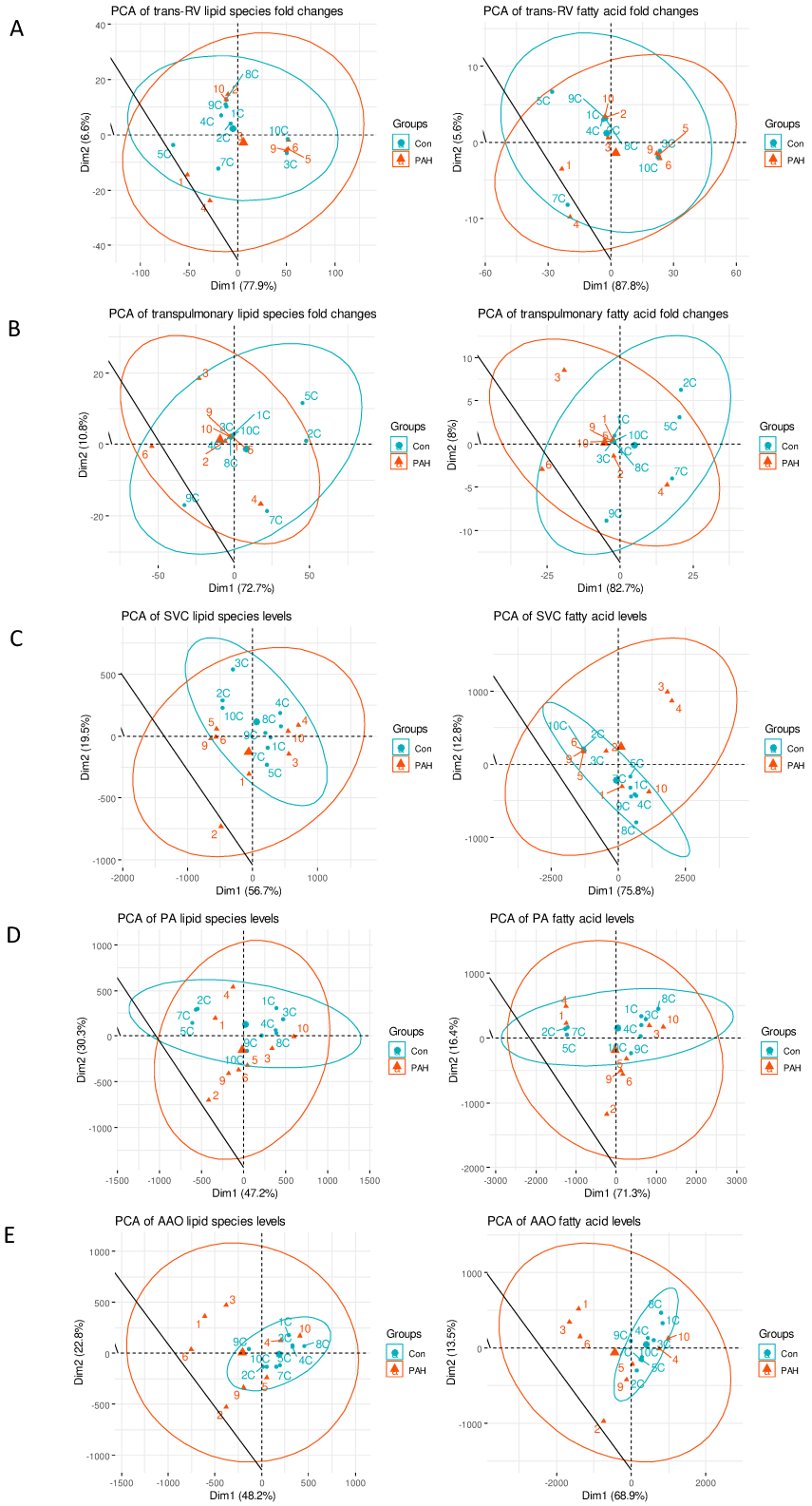

Figure S3 Principal component analysis of lipid species and fatty acid variability in each experimental setting (Lipidyzer experiments): (A) trans-RV gradient, (B) transpulmonary gradient, (C) superior vena cava, (D) pulmonary artery, (E) ascending aorta.

SUPPLEMENTAL RESULTS

Differential transpulmonary gradients (PAH vs. control) of several circulating metabolites exist and correlate with invasive hemodynamic and echocardiographic variables

We identified seven metabolites with significantly (FDR<0.15) different levels (PAH vs. control) across the pulmonary circulation (AAO vs. PA). The transpulmonary plasma concentration gradients of four of these metabolites, i.e., *N*6-acetyllysine (step up in PAH), 2-palmitoyl-GPC (16:0) (step down in PAH), *N*-acetylcarnosine (step down in PAH), and azelate (nonanedioate) (step down in PAH) along with their correlation to hemodynamic and echocardiographic variables are shown in **Fig. 4** (presented metabolites were selected based on function and effect size). These metabolites belong to amino acids (*N*6-acetyllysine), glycerophosphocholines (2-palmitoyl-GPC (16:0)), hybrid peptides (*N*-acetylcarnosine), and the group of fatty acids and their conjugates (azelate). Correlation analysis of the transpulmonary log2 fold changes of these four circulating metabolites with the key hemodynamics revealed that they had moderate to strong, positive or negative correlations with TAPSE, RVAWD, mPAP, mTPG, dTPG, mPAP/mAAO, PVRi, and other key variables (**Table S5**). Plasma concentration gradients of *N*6-acetyllysine positively correlated positively with hemodynamic indicators of PVD severity (mPAP, mTPG, dTPG, PVRi) and RV hypertrophy (RVAWD), while the levels of 2-palmitoyl-GPC (16:0) had negative correlations with the indicators of PVD severity (mRAP, mPAP, mPAP/mAAO, PVRi), hypertrophy (RVAWD), and advanced PAH with RV dilation (RVEDD). Azelate (nonanedioate) negatively correlated with fewer of the PVD severity biomarkers (mPAP, dTPG). N-acetylcarnosine had fewer correlations with the established hemodynamic biomarkers, but had the best correlation with PAWP, which is a surrogate for LVEDP and thus LV diastolic function (a LVEDP > 15 mm Hg indicates postcapillary PH (in HFpEF),[23] as opposed to pure pre-capillary PH in PAH where LVEDP is 15mmHg or less).

Finally, the lipidomics analysis of trans-pulmonary circulation revealed that phosphatidylcholines PC(FA20:5) and PC(18:0/20:5), diacylglycerol DAG(FA18:2), free fatty acid FFA(FA18:4), triacylglycerol TAG(FA20:5), and cholesterol ester CE(FA20:2) had a step-down in PAH and a step-up in controls (**Fig. 3B**).

Metabolite plasma levels of fatty acids, bile acids, glycerophosphoinositols, and amino acids are altered in PAH at the individual SVC and PA catheterization sites and correlate with invasive hemodynamic and echocardiographic variables

In order to identify global differences in levels of plasma metabolites for each site, we performed comparisons between groups (PAH vs. controls; i.e., here subjects did not serve as their own controls). Five metabolites were significantly (FDR<0.15) higher in the SVC of PAH patients vs. controls. Three of these metabolites (**Fig. 5 A,B,C**), belong to either fatty acids and conjugates (heptanoate (7:0) and caproate (6:0)) or the group of bile acids, alcohols and derivatives (glycocholenate sulfate)**.**

Heptanoate (7:0) and glycocholenate sulfate concentrations exhibited positive correlations with variables of PVD severity and RV hypertrophy (**Table S6**). Caproate also positively correlated with hemodynamic variables of PVD severity, and negatively correlated with the variables related to the LV (due to the increased LV compression in PAH) (**Table S6**).

In the PA, three metabolites were significantly (FDR<0.15) differentially concentrated, of which 1-stearoyl-GPI (18:0) and *N*6-acetyllysine had likely biologically relevant effect sizes (**Fig. 5 D,E**). 1-stearoyl-GPI (18:0), which belongs to glycerophosphoinositols, was upregulated and had moderate correlations with the PVD severity hemodynamic variables and a moderate negative correlation with the longitudinal systolic RV function variable, TAPSE (**Table S6**). *N*6-acetyllysine, an acetylated amino acid, was downregulated in PAH

and correlated negatively with the hemodynamic variables of PVD severity, hypertrophy, and advanced PAH/RV pressure overload.

SUPPLEMENTAL DISCUSSION

Trans-RV accumulation of metabolites known to drive lipotoxicity in the heart

In the Lipidyzer experiments the following LCFAs were accumulated: C14 (TAG50:5-FA14:0), C16 (TAG52:6-FA16:1 and TAG51:3-FA16:1), C18 (TAG55:3-FA18:2, **TAG54:4-FA18:0**, and TAG56:4-FA18:2), and C20 (CE20:2) (**Fig. 3A and 6**). Octadecanoic acid was not included in the Metabolon platform. However, we identified trans-RV accumulation of LCFAs represented in the Metabolon platform, namely, eicosenoate (20:1) and arachidate (20:0) (**Table S7**); however, likely due to the low sample size the arachidate FDR-adjusted p-value was above the significance threshold. Importantly, accumulated LCFAs, particularly in their saturated form, are considered to be a potent driver of lipotoxicity,[24] for example in neonatal rat ventricular myocytes.[25]

Incomplete mitochondrial β-oxidation in the hypertensive RV in PAH

Long-chain acyl-CoAs are converted to acylcarnitines by carnitine palmitoyltransferase 1 (CPT1) located at the outer mitochondrial membrane.[26] The acylcarnitines are transported into the mitochondrial matrix by the mitochondrial inner membrane transporter carnitine acylcarnitine translocase (CACT), where they are reconverted back to free carnitine and long-chain acyl-CoAs by the enzyme CPT2.[26] In the current study, we found a step-up in trans-RV stearoylcarnitine gradients in PAH and a step-down in controls (**Fig. 2E**), suggesting incomplete mitochondrial β-oxidation (i.e., lack of reconversion of stearoylcarnitine into Acyl-CoAs) in PAH. The net result is an accumulation of long-chain acylcarnitines due to incomplete β-oxidation still outpacing the tricarboxylic acid (TCA) cycle flux – a biochemical condition also found in insulin resistance.[26] A microarray mRNA expression study on postmortem RV PAH-tissue found no significant difference between CPT1, CPT2, and genes responsible for transport of acylcarnitines into mitochondria (CACT, SLC22A5) and mitochondrial β-oxidation (Acyl-CoA dehydrogenase long chain; ACADL).[27] Thus, we conclude that the trans-RV accumulation of stearoylcarnitine in our study is due to

incomplete mitochondrial β-oxidation and decreased TCA flux in response to the metabolic switch from glucose and lipid oxidation toward glycolysis (Gly).[28] Several other acylcarnitines accumulated trans-RV, shown in gray in **Fig. S4**, however not reaching the pre-selected FDR significance cutoff.

Importantly, our lipidomics experiments (Lipidyzer platform) provided additional evidence for incomplete mitochondrial β-oxidation in the hypertensive RV. While Lipidyzer cannot measure accumulation of acylcarnitines that would directly prove this point, we still observed accumulation of LCFAs. In animals LCFAs are preferentially oxidized via mitochondrial β-oxidation, while peroxisomes preferentially β-oxidize FAs not meeting the substrate range of the mitochondria, i.e., VLCFAs and branched-chain FAs.[29] There is very little complementarity between the two beta-oxidation systems: Upregulation of one β-oxidation system via pharmacological induction of peroxisome proliferator-activated receptor α (PPARα) does not compensate for loss of function of the other beta-oxidation system.[29] Therefore, the accumulation of C14 (TAG50:5-FA14:0), C16 (TAG52:6-FA16:1 and TAG51:3-FA16:1), C18 (TAG55:3-FA18:2, TAG54:4-FA18:0, and TAG56:4-FA18:2), and C20 (CE20:2) LCFAs observed in our lipidomics experiments further supports our conclusion about compromised mitochondrial β-oxidation in the hypertensive RV (**Fig S4**).

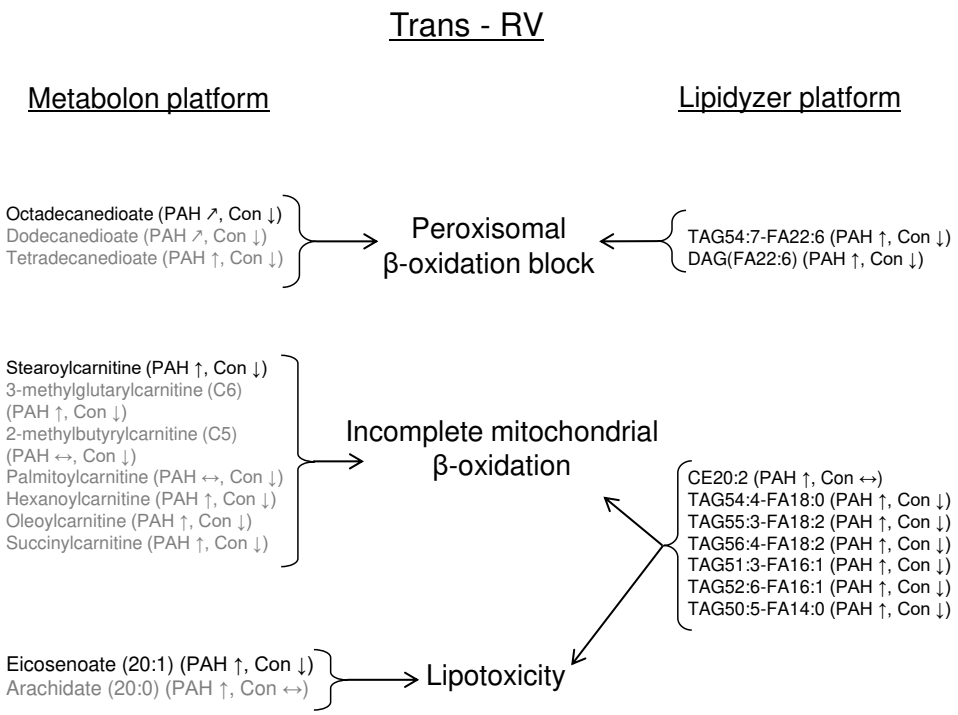

Figure S4 Metabolomics and lipidomics analyses confirm disruption of peroxisomal and mitochondrial β-oxidation and lipotoxicity in the hypertensive RV of PAH patients. Two separate studies of slightly different cohorts of PAH patients and non-PAH controls confirm the same pathological processes. Here we show metabolites used as evidence in our conclusion of: i) peroxisomal β-oxidation block (accumulation of dicarboxylic acids and very-long-chain fatty acids); ii) incomplete mitochondrial β-oxidation (accumulation of acylcarnitines and long-chain fatty acids typically oxidized via mitochondrial β-oxidation); and iii) lipotoxicity (accumulation of long-chain fatty acids). The metabolites shown in gray font had FDR-adjusted p-values greater than the preselected cutoff (0.15). The arrows show the direction of change in concentrations (PA vs. SVC). Abbreviations: DAG, diacylglycerol; TAG, triacylglycerol; CE, cholesterol ester; FDR, false discovery rate.

Accumulation of lysophospholipids across the right ventricle (Trans-RV)

1-palmitoyl-GPE (16:0) is a lysophospholipid involved in phospholipid biosynthesis by producing glycerylphosphorylethanolamine, which is known to act as a growth stimulant in hepatocytes.[30] We found a significant trans-RV step-up in PAH and a step-down in controls of 1-palmitoyl-GPE (16:0) (**Fig. 2A**) that likely indicate increased release from the hypertensive, hypertrophied RV in PAH. The trans-RV step up of 1-palmitoyl-GPE (16:0) (2.3 fold) was pronounced and probably represents boosted production within cardiac myocytes and fibroblasts, followed by release into the blood stream. We speculate that the observed accumulation (differential metabolism) of lysophospholipids (1-oleoyl-GPE 18:1 also had a step-up of 1.48 fold; **Table S4**) is indicative of a dominant phospholipid catabolism perhaps in conjunction with impaired biosynthesis of phospholipids in the hypertensive RV. Interestingly, it has been shown that lysophospholipids accumulate in ischemic myocardium of dog hearts in conditions of no collateral flow or inflammatory cell infiltration.[31] Capillary rarefaction and decreased right coronary artery perfusion pressure are the factors that trigger ischemic conditions in the hypertrophied RV of PAH patients.[32]

Trans-RV PAH-specific lipid TAG54:4-FA18:0 is associated with incidence of cardiovascular disease (CVD)

Based on 685 plasma samples from the prospective population-based Bruneck study (2000–2010, n=90 events), several lipid species were associated with CVD-related mortality (myocardial infarction, ischemic stroke, and sudden cardiac death).[33] Importantly, we found one of the CVD-associated lipids TAG54:4-FA18:0 in our trans-RV measurements (step-up in PAH, step-down in controls). A few other CVD-associated lipids varied only in the number of double bonds with the following lipids that we identified in our trans-RV experiments: TAG52:6-FA16:1, TAG50:5-FA14:0, and CE20:2.

Transpulmonary circulation (trans-PC) metabolite gradients in pediatric pulmonary arterial hypertension

In the transpulmonary plasma measurements, differential gradients of several metabolites were identified for the first time, most notably a trans-PC step-down for N6-acetyllysine and azelate (**Fig. 4A** and 4**D**). In contrast, the phosphatidylcholines PC(FA20:5) and PC(18:0/20:5) decreased in PAH but increased in controls trans-PC (**Fig. 2B**).

***N*6-acetyllysine** is an amino acid involved in lysine acetylation, which weakens histone-DNA or nucleosome-nucleosome interactions, causing conformational changes and destabilization of the nucleosome.[34] Across the pulmonary circulation (AAO vs. PA), *N*6-acetyllysine had a step-up in PAH and a step-down in controls (**Fig. 4A**). Increased serum levels of *N*6-acetyllysine have been reported to be associated with CVD-related mortality.[11] Moreover, *N*6-acetyllysine has been shown to be upregulated in monocrotalin-exposed rat lung tissue (PH animal model)[35]. Thus, the likely mechanism of transpulmonary step-up of *N*6-acetyllysine levels in our PAH patients is an increased release from the rather than the reduced uptake into the lung.

Azelate (nonanedioate), a C9 dicarboxylic acid, is involved in lipid metabolism, lipid transport, and serves as an energy source.[34] PAH patients had 48% higher azelate concentrations in venous blood plasma than controls.[36] Moreover, azelate levels positively correlated with the glycolytic rate in murine hearts [37], a mechanism that may also be particularly relevant in PAH vascular smooth muscle cells (SMCs). Previously, we unraveled in human pulmonary arterial SMCs (HPASMCs) the opposing roles of transforming growth factor beta (TGFβ1) and peroxisome proliferator-activated receptor gamma (PPARγ) in glucose metabolism and cell proliferation.[38] Particularly, upregulation of platelet isoform of phosphofructokinase (PFKP) by TGFβ1 in HPASMCs promotes vascular SMC glycolysis in human PAH.[38] In addition, glycolysis is significantly upregulated in the PAH lung.[39] Transpulmonary gradients of azelate (nonanedioate) showed a step-down in PAH and a step-up in controls (**Fig. 4G**). Therefore, we speculate that lower levels of azelate

(nonanedioate) in the pulmonary vasculature/parenchyma/interstitium are associated with a healthy, non-hypertensive phenotype; if true, this would suggests that the observed transpulmonary step-down of plasma azelate (nonanedioate) in PAH is due to its increased uptake into the lung (causing higher levels in the pulmonary vasculature (cells constituting the vascular wall) and the non-vascular lung parenchyma/interstitium).

The **phosphatidylcholines** PC(FA20:5) and PC(18:0/20:5) decreased in PAH, but increased in controls, transpulmonary circulation (AAO vs. PA; **Fig. 3B**). Phosphatidylcholine is the principal phospholipid known as a major source for the production of arachidonic acid (AA).[40] AA is a fatty acid (20:4), which is normally acetylated in membrane phospholipids.[41] AA is liberated primarily by a cytosolic phospholipase A_2 and, via actions of cyclo-oxygeanse (COX) and prostacyclin synthase, is involved in production of prostacyclin (PGI_2) [41] that inhibits platelet activation and is also a very effective vasodilator. Importantly, prostacyclin is a powerful cardioprotective hormone released by the endothelial cells, maintains equilibrium with other vasoactive hormones; violation of this equilibrium can result in CVDs such as PAH.[41]

Differential same-site metabolite concentration levels in pediatric pulmonary arterial hypertension

In the same-site (between-group) comparisons (**Fig. 5**), glycocholenate sulfate was upregulated in the SVC in PAH plasma. Glycocholenate sulfate is known to be associated with atrial fibrillation in serum of African-Americans.[42] *N*6-acetyllysine (downregulated in the PA in PAH plasma) is associated with CVD mortality as discussed above.

Metabolite gradients correlate with hemodynamic and echocardiographic variables in PAH

The pediatric values of echocardiography/hemodynamic variables (partly extrapolated from adults) that define a high risk PAH patient are: TAPSE<10 mm Hg (for children older than one year), mPAP/mAAO>0.75, PVRi>15 WU·m^2, among other criteria[2] Importantly, the alterations of novel circulating metabolite biomarkers for PAH identified in our study correlated with several of prognostic invasive hemodynamic and echocardiographic variables that are essential to diagnosis, prognosis, and outcome in PAH (**Tables 2, S4, S5,** and **S6**), as reported in the new pediatric PAH risk score.[17]

Limitations of the study

We followed strict enrollment criteria for pediatric patients undergoing invasive catheterization (see methods). As a result, we have relatively small sample sizes. Furthermore, to increase robustness of our data, we excluded measurements with a missing value in at least one of the three catheterization sites (due to very low concentrations or technical issues). Therefore, we could only unravel the metabolites with large enough concentration gradient difference (**Fig. 2 - 4**) or concentration difference (e.g., PAH SVC vs. Con SVC, **Fig. 5**) (i.e., sufficient effect size) to still produce significantly low p-values. However, because the EDTA blood samples were taken from all three catheterization sites within one minute, the design of our gradient analyses allowed us to use each patient as their own control, thereby eliminating between-patient variability and increasing the statistical power. Additionally, healthy pediatric controls are not available for a cardiac catheterization studies for ethical reasons; therefore, we used well-matched, non-PAH patients with mild to moderate LVOTO and indication for cardiac catheterization as controls. As mentioned earlier, based on our metabolite level measurements alone, it is not possible to determine which mechanism (differential release or differential uptake) is driving any step-up or a step-down in the metabolite concentration gradients. Due to the low sample size, we could not estimate the semiquantitative association of the metabolite levels with severity of PAH (WHO functional classes), however, WHO functional class and 6 minute walk distances are difficult to determine in smaller children and thus of limited value in this setting. Further preclinical and prospective clinical studies are needed to explore the biological role and clinical importance of the identified metabolites in the systemic and pulmonary circulation, and in cardiovascular cells (EC, SMC, cardiomyocytes, fibroblasts, and immune cells).

References

1 Apitz C, Hansmann G, Schranz D. Hemodynamic assessment and acute pulmonary vasoreactivity testing in the evaluation of children with pulmonary vascular disease. Expert consensus statement on the diagnosis and treatment of paediatric pulmonary hypertension. The European Paediatric Pulmonary Vascular Disease Network, endorsed by ISHLT and DGPK. *Heart* 2016;**102 Suppl 2**:ii23-ii9.

2 Hansmann G. Pulmonary hypertension in infants, children, and young adults. *J Am Coll Cardiol* 2017;**69**:2551-69.

3 Koestenberger M, Apitz C, Abdul-Khaliq H, et al. Transthoracic echocardiography for the evaluation of children and adolescents with suspected or confirmed pulmonary hypertension. Expert consensus statement on the diagnosis and treatment of paediatric pulmonary hypertension. The European Paediatric Pulmonary Vascular Disease Network, endorsed by ISHLT and DGPK. *Heart* 2016;**102 Suppl 2**:ii14-ii22.

4 Galie N, Humbert M, Vachiery JL, et al. 2015 ESC/ERS Guidelines for the diagnosis and treatment of pulmonary hypertension: The Joint Task Force for the Diagnosis and Treatment of Pulmonary Hypertension of the European Society of Cardiology (ESC) and the European Respiratory Society (ERS): Endorsed by: Association for European Paediatric and Congenital Cardiology (AEPC), International Society for Heart and Lung Transplantation (ISHLT). *Eur Heart J* 2016;**37**:67-119.

5 Selimovic N, Bergh CH, Andersson B, et al. Growth factors and interleukin-6 across the lung circulation in pulmonary hypertension. *Eur Respir J* 2009;**34**:662-8.

6 Melenovsky V, Al-Hiti H, Kazdova L, et al. Transpulmonary B-type natriuretic peptide uptake and cyclic guanosine monophosphate release in heart failure and pulmonary hypertension: the effects of sildenafil. *J Am Coll Cardiol* 2009;**54**:595-600.

7 Fares WH, Ford HJ, Ghio AJ, et al. Safety and feasibility of obtaining wedged pulmonary artery samples and differential distribution of biomarkers in pulmonary hypertension. *Pulm Circ* 2012;**2**:477-82.

8 Meoli DF, Su YR, Brittain EL, et al. The transpulmonary ratio of endothelin 1 is elevated in patients with preserved left ventricular ejection fraction and combined pre- and post-capillary pulmonary hypertension. *Pulm Circ* 2018;**8**:2045893217745019.

9 Rhodes CJ, Ghataorhe P, Wharton J, et al. Plasma Metabolomics Implicates Modified Transfer RNAs and Altered Bioenergetics in the Outcomes of Pulmonary Arterial Hypertension. *Circulation* 2017;**135**:460-75.

10 Lewis GD, Ngo D, Hemnes AR, et al. Metabolic Profiling of Right Ventricular-Pulmonary Vascular Function Reveals Circulating Biomarkers of Pulmonary Hypertension. *J Am Coll Cardiol* 2016;**67**:174-89.

11 Huang J, Weinstein SJ, Moore SC, et al. Serum Metabolomic Profiling of All-Cause Mortality: A Prospective Analysis in the Alpha-Tocopherol, Beta-Carotene Cancer Prevention (ATBC) Study Cohort. *American journal of epidemiology* 2018.

12 Hansmann G, Koestenberger M, Alastalo T, et al. 2019 Updated Consensus Statement on the Diagnosis and Treatment of Pediatric Pulmonary Hypertension. The European Pediatric Pulmonary Vascular Disease Network (EPPVDN), endorsed by AEPC, ESPR and ISHLT. *J Heart Lung Transplant* 2019;**(in press)**.

13 Simonneau G, Montani D, Celermajer DS, et al. Haemodynamic definitions and updated clinical classification of pulmonary hypertension. *Eur Respir J* 2019;**53**.

14 Rosenzweig EB, Abman SH, Adatia I, et al. Paediatric pulmonary arterial hypertension: updates on definition, classification, diagnostics and management. *Eur Respir J* 2019;**53**.

15 Abman SH, Hansmann G, Archer SL, et al. Pediatric Pulmonary Hypertension: Guidelines From the American Heart Association and American Thoracic Society. *Circulation* 2015;**132**:2037-99.

16 Hansmann G, Apitz C, Abdul-Khaliq H, et al. Executive summary. Expert consensus statement on the diagnosis and treatment of paediatric pulmonary hypertension. The European Paediatric

Pulmonary Vascular Disease Network, endorsed by ISHLT and DGPK. *Heart* 2016;**102 Suppl 2**:ii86-ii100.
17 Hansmann G, Koestenberger M, Alastalo TP, et al. 2019 updated consensus statement on the diagnosis and treatment of pediatric pulmonary hypertension: The European Pediatric Pulmonary Vascular Disease Network (EPPVDN), endorsed by AEPC, ESPR and ISHLT. *J Heart Lung Transplant* 2019;**38**:879-901.
18 Lintonen TP, Baker PR, Suoniemi M, et al. Differential mobility spectrometry-driven shotgun lipidomics. *Anal Chem* 2014;**86**:9662-9.
19 Ubhi BK. Direct Infusion-Tandem Mass Spectrometry (DI-MS/MS) Analysis of Complex Lipids in Human Plasma and Serum Using the Lipidyzer Platform. *Methods Mol Biol* 2018;**1730**:227-36.
20 Lepropre S, Kautbally S, Octave M, et al. AMPK-ACC signaling modulates platelet phospholipids and potentiates thrombus formation. *Blood* 2018;**132**:1180-92.
21 Fox J, Weisberg S. *An R Companion to Applied Regression*. Sage 2019.
22 Li J, Ji L. Adjusting multiple testing in multilocus analyses using the eigenvalues of a correlation matrix. *Heredity* 2005;**95**:221-7.
23 Lam CSP, Voors AA, de Boer RA, et al. Heart failure with preserved ejection fraction: from mechanisms to therapies. *Eur Heart J* 2018;**39**:2780-92.
24 Drosatos K, Schulze PC. Cardiac lipotoxicity: molecular pathways and therapeutic implications. *Curr Heart Fail Rep* 2013;**10**:109-21.
25 de Vries JE, Vork MM, Roemen TH, et al. Saturated but not mono-unsaturated fatty acids induce apoptotic cell death in neonatal rat ventricular myocytes. *J Lipid Res* 1997;**38**:1384-94.
26 Schooneman MG, Vaz FM, Houten SM, et al. Acylcarnitines: reflecting or inflicting insulin resistance? *Diabetes* 2013;**62**:1-8.
27 Brittain EL, Talati M, Fessel JP, et al. Fatty Acid Metabolic Defects and Right Ventricular Lipotoxicity in Human Pulmonary Arterial Hypertension. *Circulation* 2016;**133**:1936-44.
28 Legchenko E, Chouvarine P, Borchert P, et al. PPARgamma agonist pioglitazone reverses pulmonary hypertension and prevents right heart failure via fatty acid oxidation. *Sci Transl Med* 2018;**10**.
29 Schrader M, Costello J, Godinho LF, et al. Peroxisome-mitochondria interplay and disease. *J Inherit Metab Dis* 2015;**38**:681-702.
30 Jewison T, Su Y, Disfany FM, et al. SMPDB 2.0: big improvements to the Small Molecule Pathway Database. *Nucleic Acids Res* 2014;**42**:D478-84.
31 Steenbergen C, Jennings RB. Relationship between Lysophospholipid Accumulation and Plasma-Membrane Injury during Total Invitro Ischemia in Dog Heart. *Journal of molecular and cellular cardiology* 1984;**16**:605-21.
32 Ryan JJ, Archer SL. The right ventricle in pulmonary arterial hypertension: disorders of metabolism, angiogenesis and adrenergic signaling in right ventricular failure. *Circ Res* 2014;**115**:176-88.
33 Stegemann C, Pechlaner R, Willeit P, et al. Lipidomics profiling and risk of cardiovascular disease in the prospective population-based Bruneck study. *Circulation* 2014;**129**:1821-31.
34 Wishart DS, Feunang YD, Marcu A, et al. HMDB 4.0: the human metabolome database for 2018. *Nucleic Acids Research* 2018;**46**:D608-D17.
35 Rafikova O, Meadows ML, Kinchen JM, et al. Metabolic Changes Precede the Development of Pulmonary Hypertension in the Monocrotaline Exposed Rat Lung. *PLoS One* 2016;**11**:e0150480.
36 Bujak R, Mateo J, Blanco I, et al. New Biochemical Insights into the Mechanisms of Pulmonary Arterial Hypertension in Humans. *Plos One* 2016;**11**.
37 Gibb AA, Epstein PN, Uchida S, et al. Exercise-Induced Changes in Glucose Metabolism Promote Physiological Cardiac Growth. *Circulation* 2017;**136**:2144-57.
38 Calvier L, Chouvarine P, Legchenko E, et al. PPARgamma Links BMP2 and TGFbeta1 Pathways in Vascular Smooth Muscle Cells, Regulating Cell Proliferation and Glucose Metabolism. *Cell Metab* 2017;**25**:1118-34 e7.

39 Zhao Y, Peng J, Lu C, et al. Metabolomic heterogeneity of pulmonary arterial hypertension. *PLoS One* 2014;**9**:e88727.
40 Wong JT, Chan M, Lee D, et al. Phosphatidylcholine metabolism in human endothelial cells: modulation by phosphocholine. *Mol Cell Biochem* 2000;**207**:95-100.
41 Mitchell JA, Ahmetaj-Shala B, Kirkby NS, et al. Role of prostacyclin in pulmonary hypertension. *Glob Cardiol Sci Pract* 2014;**2014**:382-93.
42 Alonso A, Yu B, Qureshi WT, et al. Metabolomics and Incidence of Atrial Fibrillation in African Americans: The Atherosclerosis Risk in Communities (ARIC) Study. *PLoS One* 2015;**10**:e0142610.

Table S1 Demographics, diagnosis, and medication of IPAH patients and controls (Metabolon)

ID	Age category	Weight (kg)	BSA (m^2)	WHO Class	Diagnosis	Medication
Non-PAH Controls						
1C	Toddler	11.6	0.51	1	Moderate AS, moderate AR	VIT D3, IRO
2C	Infant	6.5	0.33	1	Mediastinal teratoma, no chemotherapy, AAO stenosis	-
3C	Adolescent	38.0	1.31	1	Severe vAS, mild AR	ASS
4C	Adolescent	56.0	1.75	1	Moderate vAS, moderate AR	LIS, MET, FSA
5C	Child	29.0	1.05	1	Moderate vAS, moderate AR	ASS
6C	Infant	3.8	0.32	1	Severe sAS, AO-Arch-Hypoplasia, imbalanced AV canal, L-SVC, no shunt	PPO, SPI, CLG
7C	Toddler	12.7	0.53	1	Moderate vAS, trivial AR	VIT C
8C	Child	32	1.05	1	Portal vein stenosis s/p liver transplantation	TAC, VIT D3, MG, ASS, PRED, IRO
PAH Patients						
1	Child	20.0	0.78	2	PAH, PDA (IPAH or young Eisenmenger)	SIL, BOS, **ILO**, SPI, ASS
2	Pre-school	12.0	0.55	2	IPAH	SIL, BOS, ASA
3	Adolescent	26.6	1.05	2	IPAH	SIL, BOS, **ILO**, DIG, PRED, PPI
4	Adolescent	67	1.75	3	APAH-CHD (repaired AP window)	SIL, BOS, **ILO**, SPI, PIO, IRO, BCP
5	Adolescent	58.0	1.61	3	PAH, Abernethy syndrome, AGS	SIL, **ILO,** HYC, RAP, VIT D3, VIT K, RET, KI, LAC, RIF
6	Adolescent	36.4	1.25	3	Portopulmonary hypertension (portal vein thrombosis)	SIL, BOS, **ILO**, PPI, UDC, SPI, ITB, FUR, VIT D3, SAL, PEN, IBU, MET
7	Infant	6.6	0.33	2	PAH, Trisomy 21, PFO, IVS	SIL, VIT D3, BOS, IRO, SPI, MG, AML, O_2
8	Infant	4.5	0.28	4	PAH, Trisomy 21, AVSD after correction, Tracheobronchomalacia	SIL, PHE, FUR, HCT, SPI, KI, CHH, AZI, ITB, SAB, **ILO**

BSA denotes body surface area; IPAH, idiopathic PAH (Nizza PH category 1.1); AAO, ascending aorta; AGS, adrenogenital syndrome; CLD, chronic lung disease; IVS, intact ventricular septum; L-SVC, persistent left superior vena cava; PDA, patent ductus arteriosus; subAS, subvalvular aortic stenosis; AR, aortic regurgitation; vAS, valvular aortic stenosis; PFO, patent foramen ovale; IVS, intact ventricular septum; AVSD, atrioventricular septal disease; s/p, status post; WHO, World Health Organization; **Medication:** AML, amlodipine; ASA, acetylsalicylic acid; AZI, azythromycin (P.O.); BOS, bosentan (P.O.); DIG, digoxin (P.O.); CHH, chloral hydrate; CLG, clopidogrel (P.O.); FUR, furosemide (Lasix) (P.O.); FSA, fluticasone/salmeterol ; HYC, hydrocortison; IBU, ibuprofen (P.O.); IRO, iron (P.O.); ITB, Ipratropium bromide (P.O.); KA, potassium (Rekawan); KI, potassium iodide (P.O.); LAC, lactulose (P.O.); MAC, macitentan (P.O.); MAZ, metamizol (P.O.); MEL, melatonin (P.O.); MG, magnesium (P.O.); NaCl, sodium chloride (P.O.); O_2, oxygen by nasal canula; PC, potassium citrate (P.O.); PEN, pentoxyfilline (P.O.); PHE, phenobarbital (P.O.); PPI, proton pump inhibitor (P.O.); PPO, propranolol (P.O.); PRED, prednisone (P.O.); RAP, ramipril (P.O.); RIF, rifaximin (P.O.); RIO, roicuguat (P.O.); SAB, salbutamol (P.O.); SIL, sildenafil (P.O.); SPI, spironolactone (P.O.); UDC, ursodiol; VIT C, D-Fluoretten (P.O.); VIT D3, Vigantolette (P.O.); VIT K, Knoakion (P.O.); ASA, acetylsalicylic acid; CLG, clopidogrel (P.O.); LIS, lisinopril (P.O.); MET = metoprolol (P.O.); MG, magnesium (P.O.); SPI, spironolactone (P.O.); PPO, propranolol (P.O.); TAC, Tacrolimus (P.O.). The **age categories** are defined in years as follows: (0-1): Infant, (1-3): Toddler, (3-5): Pre-school, (5-10): Child, and (10-18): Adolescent.

Table S2. Characteristics of control subjects and PAH patients studied (Lipidyzer)

	Control (non-PAH) (N = 9)	**PAH (N = 8)**	**P-value**
Demographics			
Age, years (mean, range)	9.1 (0.7 -17)	7.2 (3 - 18)	n.s.(0.4128)
Male sex, n (%)	7 (78)	3 (38)	
Height (m)	122.1 ± 14.3	131.4 ± 10.3	n.s.(0.5964)
Weight (kg)	26.1 ± 6.3	32.0 ± 7.2	n.s.(0.7000)
BSA (m^2)	0.93 ± 0.17	1.06 ± 0.16	n.s.(0.6294)
Disease subtypes (n)	mild to moderate LVOTO (7), mediastinal teratoma (1), portal vein stenosis (1)	IPAH (4), PAH-repaired CHD (2), portopulmonary PH (1), PAH (1)	
Key hemodynamics			
Cardiac catheterization			
sPAP (mm Hg)	21.3 ± 2.1	74.0 ± 9.9	0.0018
mPAP (mm Hg)	14.9 ± 1.5	61.1 ± 8.7	0.0006
dPAP (mm Hg)	9.0 ± 1.4	31.0 ± 8.1	0.0388
mPAP/mSAP	0.25 ± 0.02	0.81 ± 0.12	0.0001
mTPG (mm Hg)	6.7 ± 1.1	53.8 ± 8.5	0.0002
dTPG (mm Hg)	1.4 ± 0.6	31.4 ± 8.4	0.0113
PVRi ($WU \cdot m^2$)	1.67 ± 0.30	16.7 ± 3.6	0.0003
PVR/SVR	0.11 ± 0.02	0.82 ± 0.13	0.0006
Qpi	4.3 ± 0.31	3.72 ± 0.46	n.s.(0.1672)
Qsi	4.67 ± 0.37	3.90 ± 0.54	n.s.(0.1672)
Qp/Qs	0.93 ± 0.04	0.98 ± 0.04	n.s.(0.2359)
mRAP (mm Hg)	4.1 ± 0.8	5.8 ± 1.4	n.s.(0.4835)
Echo			
RVAWD (cm)	0.30 ± 0.03	0.74 ± 0.08	0.0002
RVEDD (cm)	1.3 ± 0.20	2.56 ± 0.24	0.0062
TAPSE (cm)	1.96 ± 0.08	1.61 ± 0.10	0.0228
LVEF (%)	74.2 ± 2.2	66.6 ± 3.7	n.s.(0.0872)

Values are presented as mean ± SEM. A Mann-Whitney U test was applied. $P < 0.05$ was considered significant. All PAH patients with repaired congenital heart disease (PAH-CHD) had the repair > 12 months prior to cardiac catheterization. Two of the PAH patients had trisomy 21 (all with PAH-repaired CHD; patient ID #7 and #8 in Table S1). BSA denotes body surface area; LVOTO, left ventricular outflow tract obstruction; IPAH, idiopathic PAH; CHD, congenital heart disease; sPAP, systolic pulmonary arterial pressure; mPAP, mean pulmonary arterial pressure; dPAP, diastolic pulmonary arterial pressure; mSAP, mean systemic arterial pressure; mTPG, mean transpulmonary pressure gradient; dTPG, diastolic transpulmonary pressure gradient; PVRi, pulmonary vascular resistance index; PVR, pulmonary vascular resistance; SVR, systemic vascular resistance; Qpi, pulmonary flow index; Qsi, systemic flow index; mRAP, mean right atrial pressure; RVAWD, right ventricular anterior wall diameter; RVEDD, right ventricular end-diastolic diameter; TAPSE, tricuspid annular plane systolic excursion; LVEF, left ventricular ejection fraction, n.s., not significant.

Table S3. Individual patient demographics, WHO functional class, diagnosis, and medication (Lipidyzer).

ID	Age category	Weight (kg)	BSA (m^2)	WHO Class	Diagnosis	Medication
Non-PAH Controls						
1C	Toddler	11.6	0.51	1	Moderate AS, moderate AR	VIT D3, IRO
2C	Infant	6.5	0.33	1	Mediastinal teratoma, no chemotherapy, AAO stenosis	-
3C	Toddler	38.0	1.31	1	Severe vAS, mild AR	ASS
4C	Adolescent	56.0	1.75	1	Moderate vAS, moderate AR	LIS, MET, FSA
5C	Child	29.0	1.05	1	Moderate vAS, moderate AR	ASS
7C	Toddler	12.7	0.53	1	Moderate vAS, trivial AR	VIT C
8C	Child	32	1.05	1	Portal vein stenosis s/p liver transplantation	TAC, VIT D3, MG, ASS, PRED, IRO
9C	Child	23.6	0.92	1	Mild vAS, moderate AR	-
10C	Child	24.5	0.94	1	Moderate AR, mild vAS	-
PAH Patients						
1	Child	20.0	0.78	2	PAH, PDA (IPAH or young Eisenmenger)	SIL, BOS, **ILO**, SPI, ASS
2	Pre-school	12.0	0.55	2	IPAH	SIL, BOS, ASA
3	Adolescent	26.6	1.05	2	IPAH	SIL, BOS, **ILO**, DIG, PRED, PPI
4	Adolescent	67	1.75	3	APAH-CHD (repaired AP window)	SIL, BOS, **ILO**, SPI, PIO, IRO, BCP
5	Adolescent	58.0	1.61	3	PAH, Abernethy syndrome, AGS	SIL, **ILO,** HYC, RAP, VIT D3, VIT K, RET, KI, LAC, RIF
6	Adolescent	36.4	1.25	3	Portopulmonary hypertension (portal vein thrombosis)	SIL, BOS, **ILO**, PPI, UDC, SPI, ITB, FUR, VIT D3, SAL, PEN, IBU, MET
9	Child	20.3	0.83	3	PH, CLD, s/p PDA closure, Filamin A mutation	SIL, BOS, SPI, oxygen
10	Pre-school	16.6	0.67	3	Severe IPAH, s/p syncope, AVT ++, excellent treatment response	SIL, MAC, SPI

BSA denotes body surface area; IPAH, idiopathic PAH (Nizza PH category 1.1); AAO, ascending aorta; AGS, adrenogenital syndrome; CLD, chronic lung disease; IVS, intact ventricular septum; L-SVC, persistent left superior vena cava; PDA, patent ductus arteriosus; subAS, subvalvular aortic stenosis; AR, aortic regurgitation; vAS, valvular aortic stenosis; PFO, patent foramen ovale; IVS, intact ventricular septum; AVSD, atrioventricular septal disease; s/p, status post; WHO, World Health Organization; **Medication:** AML, amlodipine; ASA, acetylsalicylic acid; AZI, azythromycin (P.O.); BOS, bosentan (P.O.); DIG, digoxin (P.O.); CHH, chloral hydrate; CLG, clopidogrel (P.O.); FUR, furosemide (Lasix) (P.O.); FSA, fluticasone/salmeterol ; HYC, hydrocortison; IBU, ibuprofen (P.O.); IRO, iron (P.O.); ITB, Ipratropium bromide (P.O.); KA, potassium (Rekawan); KI, potassium iodide (P.O.); LAC, lactulose (P.O.); MAC, macitentan (P.O.); MAZ, metamizol (P.O.); MEL, melatonin (P.O.); MG, magnesium (P.O.); NaCl, sodium chloride (P.O.); O_2, oxygen by nasal canula; PC, potassium citrate (P.O.); PEN, pentoxyfilline (P.O.); PHE, phenobarbital (P.O.); PPI, proton pump inhibitor (P.O.); PPO, propranolol (P.O.); PRED, prednisone (P.O.); RAP, ramipril (P.O.); RIF, rifaximin (P.O.); RIO, roicuguat (P.O.); SAB, salbutamol (P.O.); SIL, sildenafil (P.O.); SPI, spironolactone (P.O.); UDC, ursodiol; VIT C, D-Fluoretten (P.O.); VIT D3, Vigantolette (P.O.); VIT K, Knoakion (P.O.); ASA, acetylsalicylic acid; CLG, clopidogrel (P.O.); LIS, lisinopril (P.O.); MET = metoprolol (P.O.); MG, magnesium (P.O.); SPI, spironolactone (P.O.); PPO, propranolol (P.O.); TAC, Tacrolimus (P.O.). The age categories are defined in years as follows, [0-1): Infant, [1-3): Toddler, [3-5): Pre-school, [5-10): Child, and [10-19): Adolescent.

Table S4. Differential trans-RV metabolite concentration gradients (including selected gradient ratios) and their correlation with invasive hemodynamic / echocardiographic variables

Metabolite or metabolite ratio	Fold change Control	Fold change PAH	FDR-adjusted p-val	Selected hemodynamic or echocardiographic variables	r	p-val
Subclass: Glycerophosphoethanolamines *Role: Phospholipid biosynthesis, Glycerophospholipid metabolism, Lipid metabolism*						
1-palmitoyl-GPE (16:0)	0.70	2.31	0.0134	TAPSE, cm	-0.73	0.0254
				sPAP, mm Hg	0.55	0.0424
1-palmitoyl-GPE (16:0) / 1-linoleoyl-GPE (18:2)	0.61	2.18	0.0092	TAPSE, cm	-0.73	0.0258
				sPAP, mm Hg	0.53	0.0489
1-palmitoyl-GPE (16:0) / margarate (17:0)	0.55	2.02	0.0092	TAPSE, cm	-0.68	0.0632
				sPAP, mm Hg	0.54	0.0523
1-palmitoyl-GPE (16:0) / palmitate (16:0)	0.64	2.16	0.0099	TAPSE, cm	-0.67	0.0473
				sPAP, mm Hg	0.52	0.0577
1-palmitoyl-GPE (16:0) / stearate (18:0)	0.64	2.10	0.0099	TAPSE, cm	-0.71	0.0314
				sPAP, mm Hg	0.53	0.0533
1-palmitoyl-GPE (16:0) / 1-oleoyl-GPE (18:1)	0.77	1.50	0.0141	sPAP, mm Hg	0.53	0.0533
Subclass: Glycerophosphoethanolamines *Role: Phospholipid metabolism, Lipid transport, Lipid metabolism, Fatty acid metabolism*						
1-oleoyl-GPE (18:1)	0.78	1.48	0.0767	TAPSE, cm	-0.83	0.0104
				sPAP	-0.52	0.0533
Subclass: Fatty acids and conjugates *Role: Lipid transport, Lipid metabolism, Fatty acid metabolism*						
Octadecanedioate	0.77	1.09	0.0157	TAPSE, cm	-0.72	0.0444
				RVAWD, cm	0.52	0.0560
				Tricuspid valve E/A	-0.71	0.0226
				mPAP, mm Hg	0.56	0.0371
				PVRi, WU·m^2	0.54	0.0565
Subclass: Fatty acid esters *Role: Lipid transport, Lipid metabolism, Fatty acid metabolism*						
Stearoylcarnitine	0.74	1.21	0.0582	sPAP, mm Hg	0.52	0.0814

For gradient analysis, the p-values were generated using Type II Wald chi-square test (FDR<0.15). Abbreviations: FDR, false discovery rate; TAPSE, tricuspid annular plane systolic excursion; sPAP, systolic pulmonary arterial pressure; mRPA, mean right pulmonary arterial pressure; mPAP, mean pulmonary arterial pressure; PVRi, pulmonary vascular resistance index; RVAWD, right ventricular anterior wall diameter; mAAO, mean ascending aorta pressure.

Table S5. Differential transpulmonary metabolite concentration gradients and their correlation with invasive hemodynamic / echocardiographic variables

Metabolite or metabolite ratio	Fold change Control	Fold change PAH	FDR-adjusted p-val	Selected hemodynamic or echocardiographic variables	r	p-val
Subclass: Amino acids, peptides, and analogues *Role: Lysine metabolism*						
N6-acetyllysine	0.71	1.53	0.0476	TAPSE, cm	-0.94	0.0174
				RVSP, mmHg	0.63	0.0657
				RVAWD, cm	0.74	0.0090
				mPAP, mm Hg	0.78	0.0029
				mTPG, mm Hg	0.74	0.0056
				dTPG, mm Hg	0.78	0.0027
				mPAP/mAAO	0.84	0.0006
				PVRi, WU·m^2	0.73	0.0067
Subclass: Glycerophosphocholines *Role: Phospholipid metabolism, Lipid transport, Lipid metabolism, Fatty acid metabolism*						
2-palmitoyl-GPC (16:0)	1.22	0.83	0.0184	TAPSE, cm	0.86	0.0058
				RVAWD, cm	-0.53	0.0523
				RVEDD, cm	-0.53	0.0633
				mRAP, mm Hg	-0.54	0.0675
				mPAP, mm Hg	-0.47	0.0881
				mPAP/mAAO	-0.55	0.0383
				PVRi, WU·m^2	-0.51	0.0730
				PVR/SVR	-0.65	0.0296
Subclass: Hybrid peptides *Role: Free radical scavenger, Lipid peroxidation suppression*						
N-acetylcarnosine	1.05	0.72	0.0638	PAWP, mm Hg	0.75	0.0327
Subclass: Fatty acids and conjugates *Role: Lipid transport, Lipid metabolism, Fatty acid metabolism*						
Azelate (nonanedioate)	1.22	0.42	0.0006	mPAP, mm Hg	-0.68	0.0611
				dTPG, mm Hg	-0.75	0.0845

For gradient analysis, the p-values were generated using Type II Wald chi-square test (FDR<0.15). Abbreviations: FDR, false discovery rate; mPAP, mean pulmonary arterial pressure; mTPG, mean transpulmonary pressure gradient; dTPG, diastolic transpulmonary pressure gradient; mAAO, mean ascending aorta pressure; PVRi, pulmonary vascular resistance index; RVAWD, right ventricular anterior wall diameter; TAPSE, tricuspid annular plane systolic excursion; RVSP, right ventricular systolic pressure; mRAP, mean right atrial pressure; SVR, systemic vascular resistance; RVEDD, right ventricular end-diastolic diameter; PAWP, pulmonary arterial wedge pressure.

Table S6. Metabolites with differential concentrations in a single catheterization site (SVC, PA, AAO) correlated with hemodynamics

Metabolite or metabolite ratio	Catheterization site	Fold change (PAH vs control)	FDR-adjusted p-val	Selected hemodynamic or echocardiographic variables	rho	p-val
Subclass: Fatty acids and conjugates *Role: Lipid transport, Lipid metabolism, Fatty acid metabolism*						
Heptanoate (7:0)	SVC	1.91	0.0855	RVAWD, cm	0.73	0.0091
				RVSP, mm Hg	0.65	0.0666
				mPAP, mm Hg	0.66	0.0135
				mPAP/mAAO	0.61	0.0303
				PVRi, WU·m^2	0.63	0.0324
				PVR/SVR	0.72	0.0017
Caproate (6:0)	SVC	1.54	0.1499	mPAP, mm Hg	0.51	0.0761
				PVRi, WU·m^2	0.51	0.0936
Subclass: Bile acids, alcohols and derivatives *Role: Secondary bile acid metabolism*						
Glycocholenate sulfate	SVC	1.94	0.0883	RVAWD, cm	0.49	0.0750
				mPAP, mm Hg	0.49	0.0631
				mTPG, mm Hg	0.49	0.0764
				mPAP/mAAO	0.58	0.0253
Subclass: Glycerophosphoinositols *Role: Phospholipid metabolism, Lipid transport, Lipid metabolism, Fatty acid metabolism*						
1-stearoyl-GPI (18:0)	PA	3.85	0.0719	TAPSE, cm	-0.64	0.0831
				mPAP, mm Hg	0.58	0.0294
				mTPG, mm Hg	0.55	0.0500
				mPAP/mAAO	0.50	0.0721
				PVRi, WU·m^2	0.57	0.0473
1-stearoyl-GPI (18:0) / dihomo-linolenate (20:3n3 or n6)	PA	3.46	0.0012	RVAWD, cm	0.50	0.0602
				mPAP, mm Hg	0.66	0.0056
				mTPG, mm Hg	0.67	0.0063
				dTPG, mm Hg	0.59	0.0268
				mPAP/mAAO	0.66	0.0062
				PVRi, WU·m^2	0.72	0.0033
				PVR/SVR	0.68	0.0139
1-stearoyl-GPI (18:0) / dihomo-linoleate (20:2n6)	PA	3.51	0.0052	mPAP, mm Hg	0.50	0.0509
				PAWP, mm Hg	-0.55	0.0323
				mTPG, mm Hg	0.54	0.0363
				PVRi, WU·m^2	0.60	0.0195
				PVR/SVR	0.54	0.0611
1-stearoyl-GPI (18:0) / arachidonate (20:4n6)	PA	2.94	0.0072	TAPSE, cm	-0.77	0.0152
				mPAP/mAAO	0.54	0.0338
				PVRi, WU·m^2	0.53	0.0454
				PVR/SVR	0.54	0.0581
1-stearoyl-GPI (18:0) / 1-arachidonoyl-GPI (20:4)	PA	2.30	0.0098	TAPSE, cm	-0.87	0.0023
				mPAP/mAAO	0.51	0.0464
				PVRi, WU·m^2	0.48	0.0759
1-stearoyl-GPI (18:0) / 10-heptadecenoate (17:1n7)	PA	4.52	0.0102	TAPSE, cm	-0.77	0.0265
				PVRi, WU·m^2	0.52	0.0706
				PVR/SVR	0.59	0.0458
Subclass: Amino acids, peptides, and analogues *Role: Lysine metabolism*						
N6-acetyllysine	PA	0.49	0.0944	RVSP, mm Hg	-0.70	0.0311
				RVAWD, cm	-0.79	0.0023
				RVEDD, cm	-0.65	0.0208
				mPAP, mm Hg	-0.68	0.0072
				mTPG, mm Hg	-0.73	0.0045
				dTPG, mm Hg	-0.60	0.0387
				mPAP/mAAO	-0.61	0.0225
				PVRi, WU·m^2	-0.77	0.0033
				PVR/SVR	-0.72	0.0150

For between-group comparisons, Mann-Whitney U test was used, FDR<0.15. Abbreviations: FDR, false discovery rate; mPAP, mean pulmonary arterial pressure; mAAO, mean ascending aorta pressure; PVRi, pulmonary vascular resistance index; SVR, systemic vascular resistance; RVAWD, right ventricular anterior wall diameter; RVSP, right ventricular systolic pressure; mTPG, mean transpulmonary pressure gradient; TAPSE, tricuspid annular plane systolic excursion; PAWP, pulmonary arterialwedge pressure.

Table S7. Trans-RV fold changes (FC), p-values, and FDR-adjusted p-values (q-values) of the metabolites in the Discussion of the main manuscript.

Metabolite	FC PAH	FC Con	p-value	q-value
1-palmitoyl-GPE (16:0)	2.3103	0.7031	0.000636916	0.013375246
1-oleoyl-GPE (18:0)	1.4797	0.7813	0.005723868	0.07668947
octadecanedioate	1.09	0.7679	0.002980109	0.043901007
dodecanedioate	1.077	0.7227	0.04943325725	0.3245496113
tetradecanedioate	1.2715	0.84	0.2517646426	0.6765543234
TAG54:7-FA22:6	1.4449	0.7746	0.005475415	0.104955657
DAG(FA22:6)	1.4728	0.9476	0.001996479	0.041926055
eicosenoate (20:1)	1.1684	0.845	0.008598818	0.10143864
arachidate (20:0)	1.3382	0.9749	0.03300509845	0.2499439809